Human Molecular Genetics, 2003, Vol. 12, No. 5 **551–559**
DOI: 10.1093/hmg/ddg049

The voltage-gated potassium channel Kv1.3 regulates energy homeostasis and body weight

Jianchao Xu[1,5,6,†], Pandelakis A. Koni[7,8,†], Peili Wang[1,5], Guoyong Li[1,5], Leonard Kaczmarek[3,5], Yanling Wu[1,5], Yanyan Li[1,5], Richard A. Flavell[2,4,5] and Gary V. Desir[1,5,6,*]

[1]Department of Medicine, [2]Section of Immunobiology, [3]Department of Pharmacology, [4]Howard Hughes Medical Institute and [5]Yale University School of Medicine, New Haven, CT, USA, [6]VA CT Medical Center, New Haven, CT, USA, [7]Medical College of Georgia, Augusta, GA, USA and [8]RIKEN Research Center for Allergy and Immunology, Yokohama, Japan

Received November 4, 2002; Revised December 23, 2002; Accepted January 3, 2003

Voltage-gated potassium (Kv) channels regulate cell membrane potential and control a variety of cellular processes. Kv1.3 channels are expressed in several tissues and believed to participate in cell volume regulation, apoptosis, T cell activation and renal solute homeostasis. Examination of Kv1.3-deficient mice (Kv1.3$^{-/-}$), generated by gene targeting, revealed a previously unrecognized role for Kv1.3 in body weight regulation. Indeed, Kv1.3$^{-/-}$ mice weigh significantly less than control littermates. Moreover, knockout mice are protected from diet-induced obesity and gain significantly less weight than littermate controls when placed on a high-fat diet. While food intake did not differ significantly between Kv1.3$^{-/-}$ and controls, basal metabolic rate, measured at rest by indirect calorimetry, was significantly higher in knockout animals. These data indicate that Kv1.3 channels may participate in the pathways that regulate body weight and that channel inhibition increases basal metabolic rate.

INTRODUCTION

Voltage-gated potassium (Kv) channels are a diverse group of membrane proteins that regulate cell membrane potential. Kv1.3, a member of the *Shaker* family of Kv channels, is found in many tissues, including kidney (1), lymphocytes (2–6), CNS (7), liver, skeletal muscle, testis and spermatozoa (8), and osteoclasts (9,10). It may participate in a variety of cellular functions including apoptosis, cell volume regulation and T cell stimulation (3,4,11,12). Channel activity is upregulated by serum-glucocorticoid activated kinase (SGK), one of the main mediators of aldosterone's action at the renal distal tubule (13). Protein kinase C (PKC) increases (14) and tyrosine kinase (TK) inhibits Kv1.3 channel activity (15). In olfactory bulb neurons, where Kv1.3 mediates a large proportion of the measured outward current, its activity is down-regulated by insulin through activation of receptor TK (15,16). Site directed mutagenesis experiments indicate that insulin causes the phosphorylation of multiple tyrosine residues in Kv1.3.

The role of insulin signaling in the brain is not well understood (17). Brain insulin receptors are found not only in the olfactory bulb, but also in the choroid plexus, the hippocampus and the arcuate nucleus of hypothalamus. The hypothalamus expresses GLUT4, an insulin-sensitive glucose transporter and is an important area with regards to appetite control and energy expenditure (18). It integrates a variety of peripheral signals, including leptin and insulin, and relays appropriate messages to specific neurons to either increase or decrease food intake. Optimally, energy intake equals energy expenditure and the organism is able to maintain a constant body weight. Energy output can vary greatly since it consists not only of an obligatory portion sustaining cellular and organ functions (basal metabolic rate), but also of two variable components, i.e. adaptive thermogenesis and physical activity (19). There are data suggesting that the hypothalamus also modulates adaptive thermogenesis. The molecular details of these interactions are under intense investigation since the incidence of obesity has reached epidemic proportions in developed countries.

In spite of extensive data regarding the kinetic and pharmacologic properties, and regulation of Kv1.3, its physiological role(s) is not well understood. We do, however, know that the channel is expressed in the hypothalamus (20), and that it is regulated by insulin, and thus can be regarded as one of the

*To whom correspondence should be addressed at: Section of Nephrology, Department of Medicine, Yale School of Medicine, 333 Cedar Street, LMP 2073, PO Box 208029, New Haven, CT 06520-8029, USA. Tel: +1 2035062500; Fax: +1 5084628950; Email: gary.desir@yale.edu
†The authors wish it to be known that, in their opinion, the first two authors should be regarded as joint First Authors.

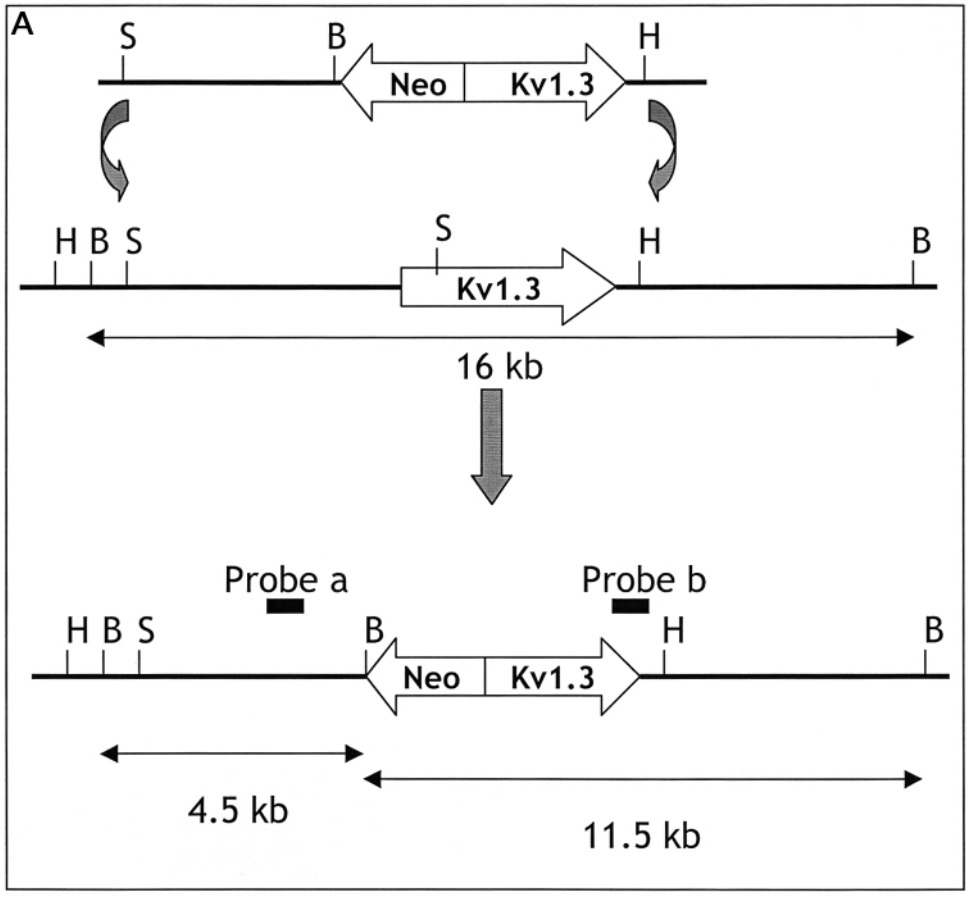

Figure 1. Generation of Kv1.3$^{-/-}$ mice. (**A**) The targeting construct deletes the *Kv1.3* promoter region and the 5′ third of the coding region, and incorporates a *Bam*HI (B) site for screening. Other endonuclease sites shown are *Hin*dIII (H) and *Sca*I (S). (**B**) Genomic DNA was amplified by PCR and a band of the expected size (340 bp) was detected in wild-type but not in Kv1.3$^{-/-}$ mice. (**C**) The Kv1.3 protein was assayed by western blotting. A band of the expected size (68–72 kDa) was detected in Kv1.3$^{+/+}$ but not in Kv1.3$^{-/-}$ mice.

insulin receptor substrates (IRS). Interestingly, mice with a neuron-specific disruption of the IR gene (NIRKO mice) developed diet-sensitive obesity with increases in body fat and plasma leptin levels, mild insulin resistance, elevated plasma insulin levels and hypertriglyceridemia, suggesting IR signaling in the CNS plays an important role in regulation of energy disposal, fuel metabolism (21). To examine the physiological role of Kv1.3 *in vivo*, especially to test whether Kv1.3 serves as IRS in body weight control and energy homeostasis, we generated Kv1.3-deficient mice (Kv1.3$^{-/-}$) by disrupting the Kv1.3 locus using homologous recombination and examined their phenotype.

RESULTS

Decreased body weight in Kv1.3$^{-/-}$ mice

Figure 1A depicts the strategy employed to disrupt the *Kv1.3* locus. Gene disruption was confirmed by PCR and western blotting (Fig. 1B and C). The expected Mendelian ratio was observed for mice born from the mating of heterozygous parents. Newborn Kv1.3$^{-/-}$ mice appeared normal, required no specific precautions for survival and growth, and were indistinguishable from wild-type (WT) littermates (Kv1.3$^{+/+}$) in terms of appearance and behavior.

Kv1.3$^{-/-}$ animals consistently weighed less than littermate controls, as illustrated in Figure 2A, where female mice were observed in metabolic cages for up to 35 days beginning at 50 days of age. The weight difference was also noted in pair-fed male mice (Fig. 2B). Body lengths were indistinguishable, as was bone structure assessed by dual-energy X-ray absorptiometry scan (DEXA). Although total body fat content estimated by DEXA was lower in Kv1.3$^{-/-}$ mice, the difference did not reach statistical significance (Table 1).

Increased basal metabolic rate in Kv1.3$^{-/-}$ mice

Body weight is controlled by the net difference between energy intake and expenditure. Therefore, we measured energy intake, metabolic rate and activity levels in Kv1.3$^{-/-}$ mice, to further elucidate the role of Kv1.3 in body weight regulation. There were no significant differences in food intake between Kv1.3$^{-/-}$ mice and control littermates. In contrast, basal metabolic rate (measured by indirect calorimetry from 11 a.m. to 4 p.m.) was significantly higher in Kv1.3$^{-/-}$ mice (Table 1). The higher in

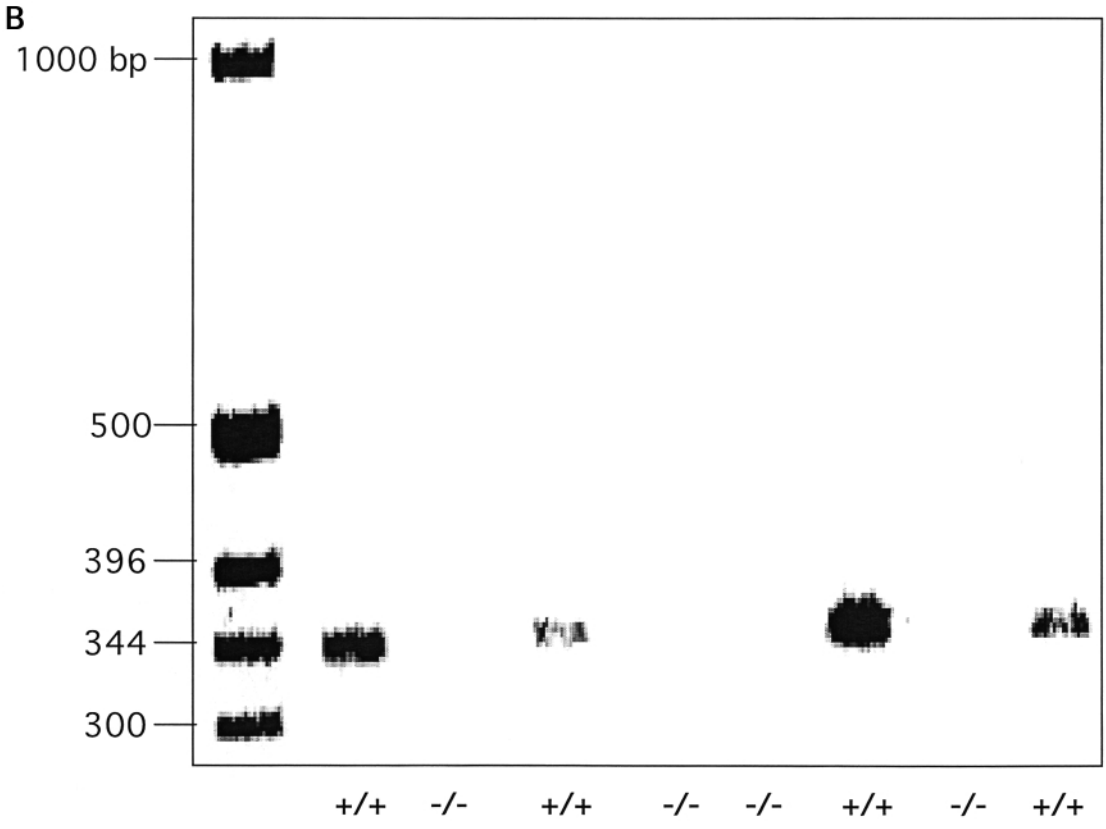

Figure 1. *continued.*

Table 1. Comparison of Kv1.3$^{+/+}$ and Kv1.3$^{-/-}$ mice on regular diet. Body weights and length, total body fat, food intake, metabolic rate and total activity were determined in Kv1.3$^{-/-}$ mice and control littermates. Percentage body fat was measured by DEXA at the Yale Core Center for Musculoskeletal Disorders (P30AR46032). Leptin and glucagon levels were measured by ELISA at Linco Research (MO, USA). Values represent the mean ± SEM

	Male Kv1.3$^{+/+}$	Male Kv1.3$^{-/-}$	*P*	Female Kv1.3$^{+/+}$	Female Kv1.3$^{-/-}$	*P*
Body weight (g), $n = 10$	26.84 ± 0.99	23.53 ± 0.36	<0.003	19.90 ± 0.64	18.30 ± 0.64	<0.05
Body length (cm), $n = 10$	9.20 ± 0.09	9.07 ± 0.02		8.47 ± 0.05	8.31 ± 0.07	
Body fat (%), $n = 10$	28.16 ± 2.08	24.90 ± 1.18		21.56 ± 3.69	19.32 ± 1.56	
Leptin (ng/ml), $n = 6$	1.92 ± 0.21	1.9 ± 0.10		2.46 ± 0.36	2.10 ± 0.36	
Food intake (g/g BW/day), $n = 8$	0.13 ± 0.01	0.15 ± 0.01		0.13 ± 0.003	0.14 ± 0.008	
Glucagon (pg/ml), $n = 6$	84.30 ± 8.54	76.50 ± 18.50				
Metabolic rate (cal/h/g), $n = 4$	11.80 ± 0.31	13.90 ± 0.39	<0.0005			
Total activity (counts/h), $n = 4$	917.00 ± 96.0	794.00 ± 57.00				

metabolic rate of Kv1.3$^{-/-}$ mice could not be explained by changes in the level of physical activity since both knockout mice and control littermates were as active during the period of observation (Table 1).

Kv1.3$^{-/-}$ mice are resistant to diet-induced obesity

We then tested whether Kv1.3 gene disruption afforded any protection against diet-induced obesity. Metabolic rate, activity levels, and caloric intake were measured in control and Kv1.3$^{-/-}$ mice exposed to a high-fat diet. As shown in Figure 3A, Kv1.3$^{-/-}$ mice gained significantly less weight than controls on a high-fat diet. The difference in weight gain was evident by the second month, reached statistical significance by the third month and persisted until the end of the observation period. The difference in weight was noted in both male and female Kv1.3$^{-/-}$ mice (Fig. 3B). While metabolic rate was significantly higher in Kv1.3$^{-/-}$ mice on a high-fat diet, basal activity level and food intake were undistinguishable (Table 2). As would be expected for obese animals, Kv1.3$^{+/+}$ mice developed hyperglycemia, in spite of a significant increase in circulating insulin level (Table 2). In contrast,

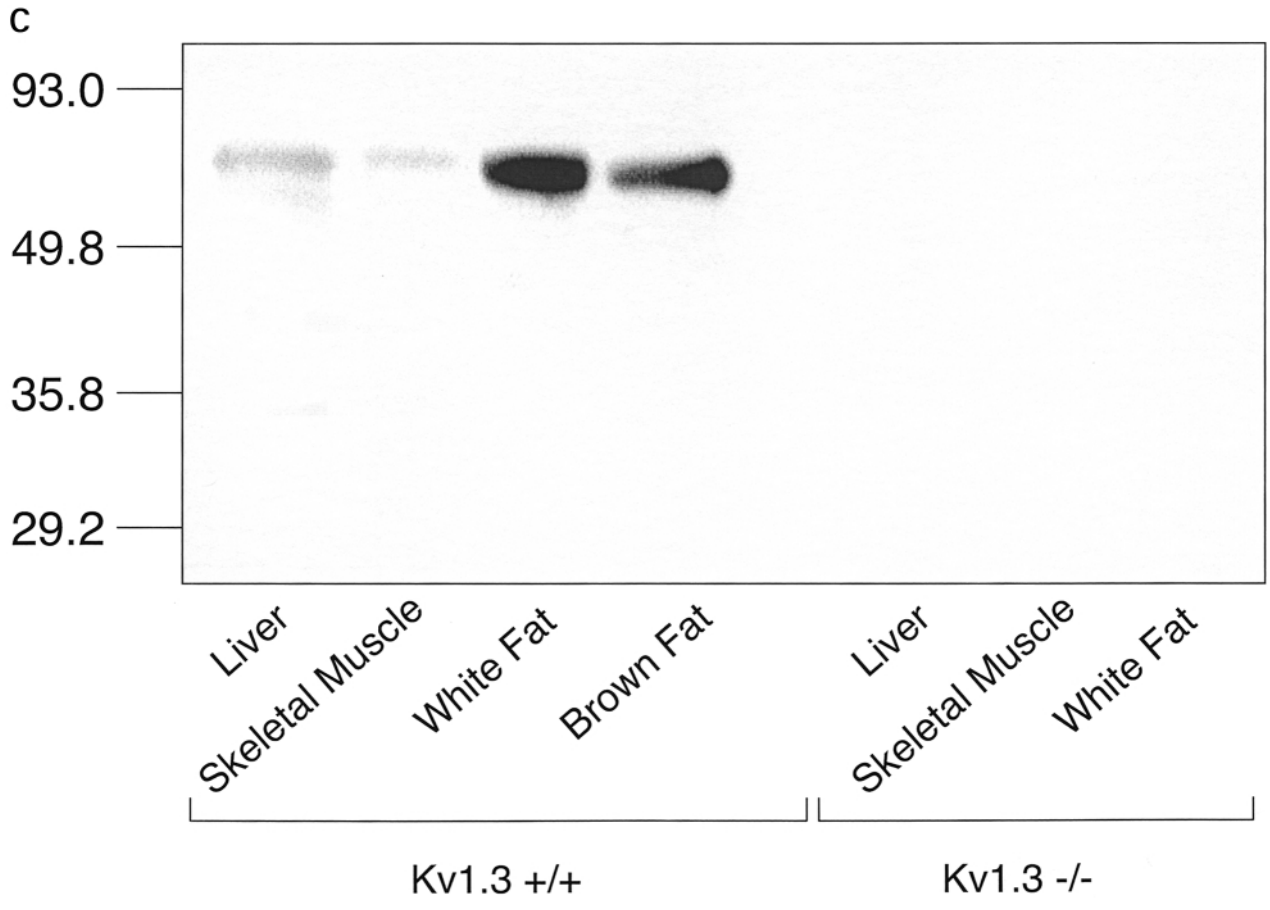

Figure 1. *continued.*

Table 2. Metabolic parameters of $Kv1.3^{+/+}$ and $Kv1.3^{-/-}$ mice on high-fat diet. Mice were placed on a high-fat diet for up to 8 months. Body weights, food intake, metabolic rate, and total activity were determined in $Kv1.3^{-/-}$ mice and control littermates. Blood glucose values were measured using a Glucometer (Bayer, West Haven, CT, USA). Insulin and glucagon levels were measured by ELISA at Linco Research (MO, USA). Values represent the mean ± SEM

	$Kv1.3^{+/+}$	$Kv1.3^{-/-}$	*P*
Body weight (g), $n = 8$	48.04 ± 2.90	39.29 ± 0.60	<0.001
Metabolic rate (cal/h/g), $n = 4$	11.06 ± 0.32	13.52 ± 0.34	<0.001
Total activity (counts/h), $n = 4$	258.75 ± 17.5	278 ± 6.70	NS
Glucose (mg%), $n = 8$	153.21 ± 13.0	108.14 ± 7.00	<0.02
Insulin (ng/ml), $n = 8$	20.05 ± 3.50	1.58 ± 0.16	<0.01
Glucagon (pg/ml), $n = 8$	129.33 ± 15.0	123.10 ± 14.20	NS

$Kv1.3^{-/-}$ maintained normal blood sugars with relatively low plasma insulin levels (Table 2).

DISCUSSION

The main finding of these studies relate to the fact that mice bearing a disrupted *Kv1.3* gene weigh significantly less that control littermates and are protected against diet-induced obesity. The decrease in body weight cannot be explained by non-specific systemic effect of gene knockout since the $Kv1.3^{-/-}$ animals could not be distinguished from control littermates by their behavior, did not require any special precautions for breeding and had a similar life expectancy (up to 18 months of observation). Moreover, since food intake of $Kv1.3^{-/-}$ mice was similar to that of littermate controls, the weight loss observed in the knockout animals could not have been caused by a decrease in energy intake.

The hypothalamus is recognized as an important component of the system that regulates energy balance and body weight (19,22). It integrates a number of peripheral signals, including leptin and insulin, and signal-specific neurons to either increase or decrease energy intake. Since food intake was not affected by *Kv1.3* disruption, Kv1.3 channel activity is unlikely to contribute importantly to the signal pathways that regulate appetite.

It is clear that inactivation of the *Kv1.3* gene leads to a significant increase in basal metabolic rate. In a steady state, energy intake equals energy expenditure and the organism is able to maintain a constant body weight. Like food intake, energy output can vary greatly. In addition to energy expenditure required for cellular and organ functions (basal metabolic rate), there are two variable components—adaptive thermogenesis and physical activity (18)—that regulate energy

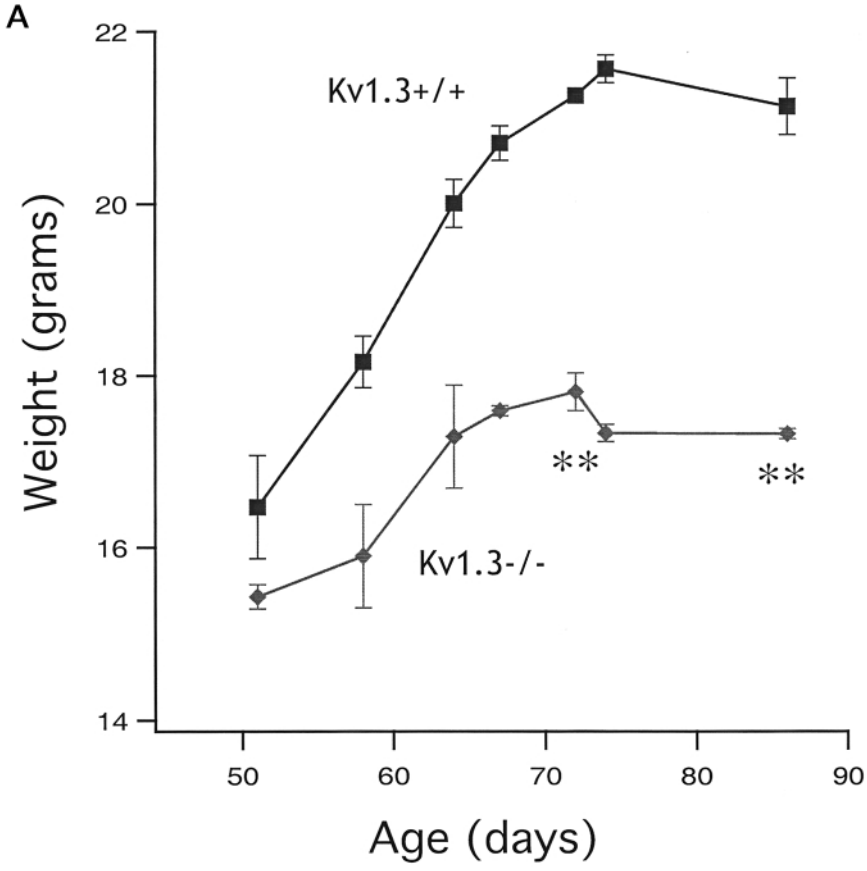

Figure 2. Kv1.3$^{-/-}$ mice weigh less than littermate controls. (**A**) Kv1.3$^{+/+}$ ($n = 5$) and Kv1.3$^{-/-}$ ($n = 5$) female animals were housed individually in metabolic cages where food intake, weight and urine output were monitored for 35 days beginning at day 50 of age. Kv1.3$^{-/-}$ mice weighed less than control mice (**$P < 0.01$). Values represent mean ± SEM. (**B**) Kv1.3$^{+/+}$ ($n = 5$) and Kv1.3$^{-/-}$ ($n = 5$) male animals were housed in communal cages and body weight was measured at 4 months of age. Kv1.3$^{-/-}$ mice weighed less than control mice (**$P < 0.01$). Values represent mean ± SEM.

output. Kv1.3$^{-/-}$ mice had the same level of physical activity as control littermates at rest, the period during which basal metabolic rate was assessed by indirect calorimetry. We therefore conclude that an increase in physical activity is unlikely to account for the observed rise in metabolic rate of Kv1.3$^{-/-}$ mice.

The fact that activity levels of Kv1.3$^{-/-}$ and control mice, measured at rest, did not differ significantly suggests that *Kv1.3* gene disruption caused the animals to generate more heat or to be less efficient in processing and storing energy supplies. Adaptive thermogenesis is a process that is regulated by the hypothalamus and mediated through the activation of the sympathetic nervous system (19). The hypothalamus senses changes either in ambient temperature or in energy intake and signals brown adipose tissue and skeletal muscle to either increase or decrease heat production. This process has obvious advantages and serves as a means of maintaining a constant body temperature in a variable environment or a constant body weight in spite of large changes in energy intake. It is conceivable that Kv1.3 is part of the system that regulates adaptive thermogenesis and that Kv1.3 gene disruption could cause an increase in heat production in the absence of changes in ambient temperature and diet. Indeed, the Kv1.3 channel protein is abundantly expressed in white and brown fat, and can be detected in skeletal muscle. Kv1.3 inhibition has been shown to depolarize cell membranes and modulates intracellular calcium and subsequent signaling events in T lymphocytes (12). Changes in Kv1.3 activity could, for instance, modulate membrane voltage and Ca^{2+} cycling in brown fat and skeletal muscle.

It should be noted that, although our data strongly support the notion that Kv1.3 channels participate in body weight regulation, they do not conclusively prove it. Since the Kv1.3$^{-/-}$ mice used in our studies were bred as B6/129 congenics, the targeted region may contain additional genes linked to the Kv1.3 locus, which could affect body weight and energy metabolism. For example, quantitative trait loci have been mapped using knockout/congenic strains (23) and mice transgenic mice over-expressing the enzyme 11B hydroxysteroid dehydrogenase type 1 are prone to developing visceral obesity, particularly when placed on a high-fat diet (24).

In conclusion, our results suggest that Kv1.3 is an important component of the pathways that regulate body weight and energy homeostasis. Kv1.3$^{-/-}$ animals weigh significantly less than control littermates, primarily because they have higher

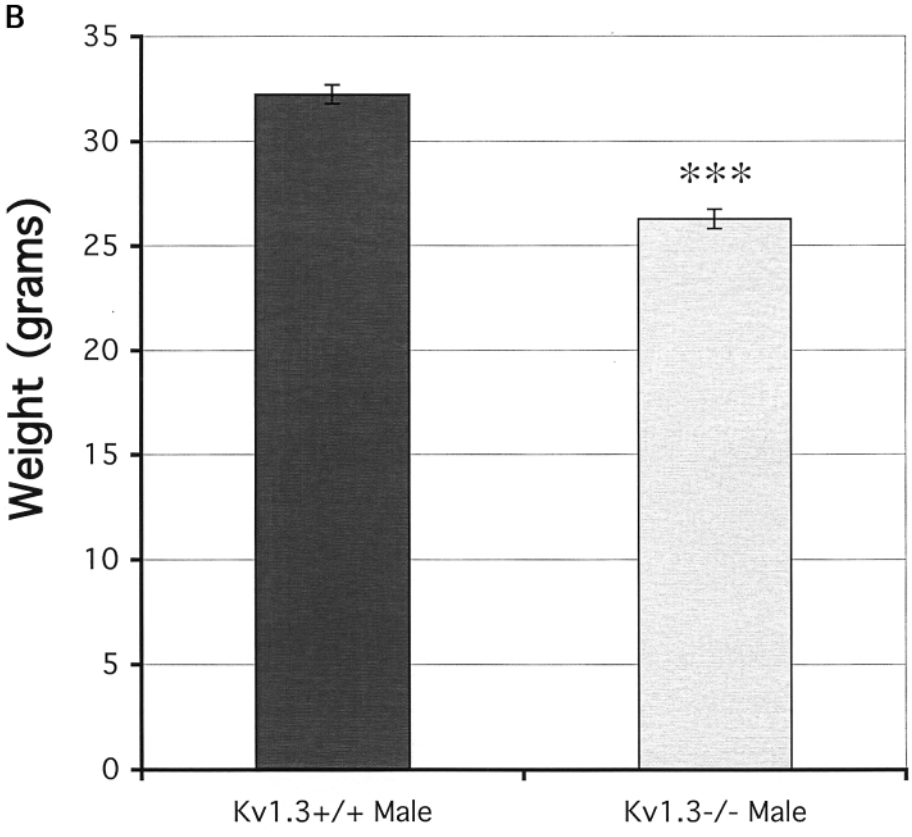

Figure 2. *continued*.

basal metabolic rates, perhaps due to an increase in thermogenesis. Further studies are needed to elucidate the exact molecular details underlying the effect of Kv1.3 on metabolic rate since the channel is expressed in the central nervous system, white and brown fat and skeletal muscle. Nonetheless, the current study highlights the potential role of Kv1.3 channels in body weight regulation, and identifies the channel and its signaling pathway as possible targets for the development of drugs useful in the management of obesity, a condition that has reached epidemic proportions in developed countries.

MATERIALS AND METHODS

Generation of Kv1.3-deficient mice

The *Kv1.3* gene was isolated from a lambda Fix II 129Sv/J library (Stratagene) using a 5′ region of the rat homolog (GenBank accession number m30441) as a probe. The identity of the clone was confirmed by restriction mapping and sequencing. The targeted region spans an 8.2 kb region between an upstream *Bam*HI site and the 3′ end of the lambda Fix II genomic clone. The *Bam*HI site was subsequently eliminated by Klenow polymerase end-filling and re-ligation. The construct was then linearized with *Xho*I by partial digestion, and a herpes simplex virus thymidine kinase gene cassette was inserted into the vector *Xho*I site at the 3′ end of the targeted region after Klenow end-filling. An *Xho*I/*Sal*I neomycin resistance cassette from pMC1neopA (Stratagene) was then inserted into the *Xho*I site 5′ of *Kv1.3* in the opposite orientation to *Kv1.3* This regenerates the *Xho*I site downstream of the neomycin resistance cassette. The 1.8 kb *Xho*I/*Sca*I region of *Kv1.3* was then excised and the construct re-ligated after Klenow end-filling. The left and right arms of the targeting construct are 4.5 and 1.8 kb, respectively.

The targeting vector (see Fig. 1A) was linearized at a *Not*I site and 25 mg was used to electroporate 107 W9.5 embryonic stem cells. Embryonic stem cells were then plated onto mitomycin C-treated embryonic fibroblasts and drug selection begun 24 h later with 2 mM gancyclovir (Syntex) and 0.3 mg/ml G418 (GIBCO-BRL). Embryonic stem cell clones and mice were screened by *Bam*HI-digest Southern blot analysis with probes a and b. Probe a is a 1.5 kb *Eco*RI region and probe b is a 0.5 kb *Hinc*II/*Sal*I fragment at the 3′ end of the genomic clone. Homologous recombinant embryonic stem cells were injected into C57BL/6 blastocysts and chimeric males were bred to C57BL/6 females. The Kv1.3$^{-/-}$ mice and control littermates used in these studies were F_{10}–F_{12} offsprings obtained from B6/129 intercrosses. All mice were housed in specific pathogen-free conditions in accordance with institutional animal care and use guidelines.

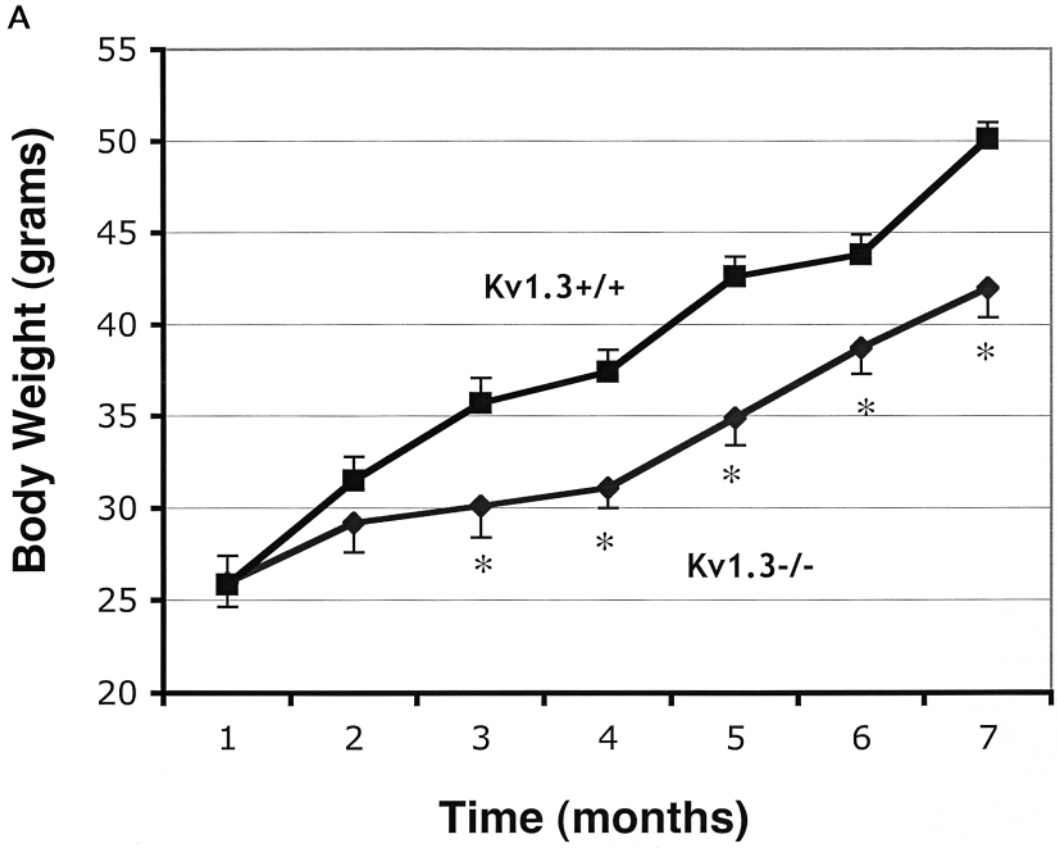

Figure 3. Kv1.3$^{-/-}$ mice are protected from diet-induced obesity. (**A**) Male Kv1.3$^{-/-}$ ($n=9$) and control ($n=9$) mice were fed with a high-fat diet (Bio-Serv F3282, 35.5% fat), and weights were determined at the indicated ages. Kv1.3$^{-/-}$ mice gained significantly less weight than Kv1.3$^{+/+}$ mice (*$P<0.05$). (**B**) Kv1.3$^{-/-}$ (five males and five females) and control (five males and five females) mice were fed with a high-fat diet (Bio-Serv F3282, 35.5% fat), and weights were determined at 7 months of age. Both male and female Kv1.3$^{-/-}$ mice gained significantly less weight than Kv1.3$^{+/+}$ mice (*$P<0.02$ and 0.03, respectively).

Western blot

Homogenates were prepared from liver, skeletal muscle, white fat and brown fat of Kv1.3$^{-/-}$ or Kv1.3$^{+/+}$ mice. Protein (10 μg) was resolved by 10% SDS–PAGE and transferred to a nitrocellulose membrane, which was probed with a rabbit anti-human Kv1.3 polyclonal antibody (1:200; Santa Cruz Biotechnology Inc.).

PCR

Genomic DNA was amplified by the polymerase chain reaction (PCR) using Kv1.3 specific primers (5′ primer is ATACTTCGACCCGCTCCGCAATGA, 3′ GCAGAAGATGACAATGGAGATGAG), denaturing at 94°C for 1 min, annealing at 55°C for 2 min and extension at 68°C for 3 min, 35 cycles.

Dual-energy X-ray absorptiometry scan

Whole body composition was analyzed by DEXA (PIXImus, GE-Lunar, CT, USA). Mice were anesthetized with ketamine and xylazine. Accuracy was determined using phantoms of known values. Correlation of lean tissue mass of the total body was excellent ($r^2=0.99$), as were the smaller components of fat mass and bone mass ($r^2=0.86$ and $r^2=0.92$, respectively). The machine is precise with the mean intra-individual coefficient of variation of 1.60% for bone mineral content and 0.84% for bone mineral density. Total body analysis was acquired in 5 min and the data were analyzed using software provided by the manufacturer.

Measurement of metabolic rate and activity levels

Mice were housed in a quiet room at an ambient temperature of 24°C. Metabolic rate was measured by indirect calorimetry using a four-chamber Oxymax system (Columbus Instruments, Columbus, OH, USA), an indirect, open-circuit calorimeter. O_2 consumption and CO_2 production were measured every 40 min for up to 48 h. Heat production was calculated and expressed per gram body weight (cal/h/g BW). The measurements obtained over the 5 h period (11 a.m.–4 p.m.) on two consecutive days were averaged. Activity levels were assessed simultaneously using the optical beam technique using an Opto-Varimex Mini (Columbus Instruments, Columbus, OH, USA).

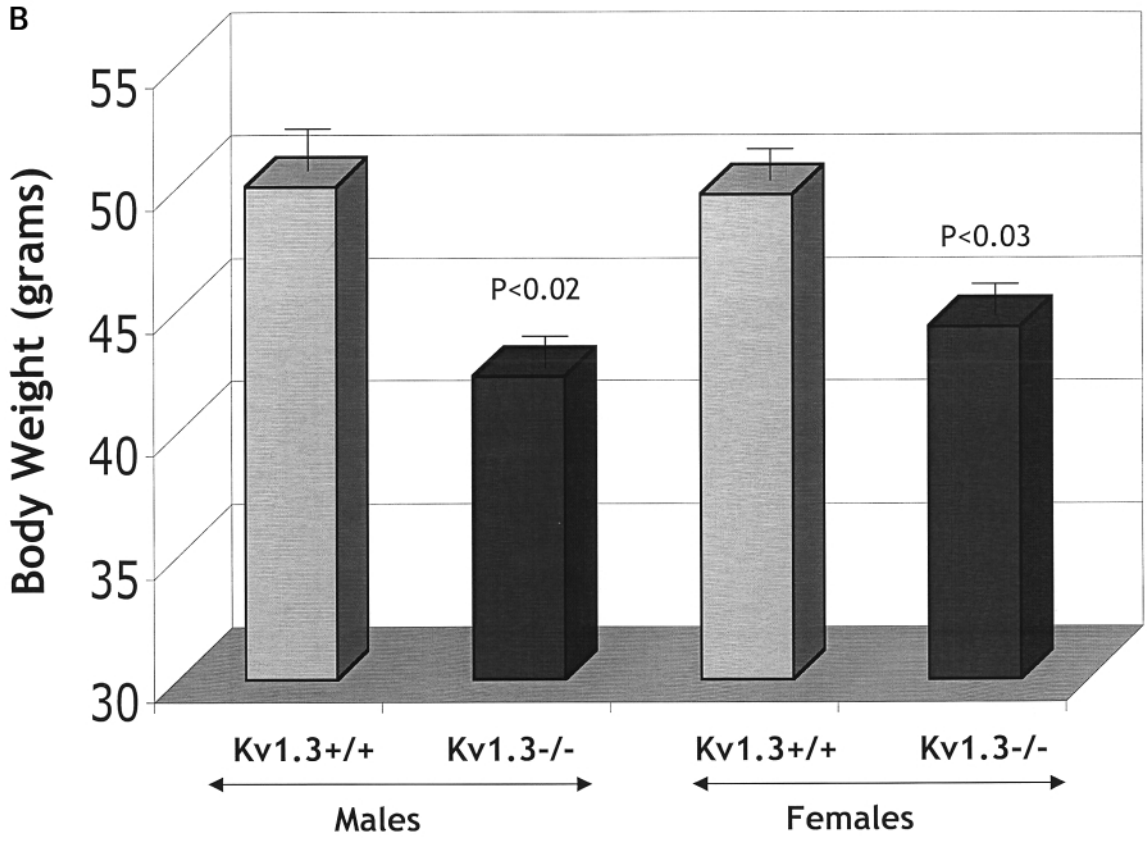

Figure 3. *continued*.

REFERENCES

1. Yao, X., Chang, A.Y., Boulpaep, E.L., Segal, A.S. and Desir, G.V. (1996) Molecular cloning of a glibenclamide-sensitive, voltage-gated potassium channel expressed in rabbit kidney. *J. Clin. Invest.*, **97**, 2525–2533.
2. Cahalan, M.D., Chandy, K.G. and Grissmer, S. (1991) Potassium channels in development, activation and disease in T lymphocytes. *Curr. Top. Membranes*, **39**, 357–394.
3. Attali, B., Romey, G., Honoré, E., Schmid-Alliana, A., Mattéi, M.-G., Lesage, F., Ricard, P., Barhanin, J. and Lazdunski, M. (1992) Cloning, functional expression, and regulation of two K^+ channels in human T lymphocytes. *J. Biol. Chem.*, **267**, 8650–8657.
4. Attali, B., Honoré, E., Lesage, F., Lazdunski, M. and Barhanin, J. (1992) Regulation of a major cloned voltage-gated K^+ channel from human T lymphocytes. *FEBS Lett.*, **303**, 229–232.
5. Ghanshani, S., Wulff, H., Miller, M.J., Rohm, H., Neben, A., Gutman, G.A., Cahalan, M.D. and Chandy, K.G. (2000) Up-regulation of the IKCa1 potassium channel during T-cell activation. Molucular mechanisms and functional consequences. *J. Biol. Chem.*, **275**, 37137–37149.
6. Levite, M., Cahalon, L., Peretz, A., Hershkoviz, R., Sobko, A., Ariel, A., Desai, R., Attali, B. and Lider, O. (2000) Extracellular K(+) and opening of voltage-gated potassium channels activate T cell integrin function: physical and functional association between Kv1.3 channels and beta1 integrins. *J. Exp. Med.*, **191**, 1167–1176.
7. Mourre, C., Chernova, M.N., Martin-Eauclaire, M.F., Bessone, R., Jacquet, G., Gola, M., Alper, S.L. and Crest, M. (1999) Distribution in rat brain of binding sites of kaliotoxin, a blocker of Kv1.1 and Kv1.3 alpha-subunits. *J. Pharmac. Exp. Ther.*, **291**, 943–952.
8. Jacob, A., Hurley, I.R., Goodwin, L.O., Cooper, G.W. and Benoff, S. (2000) Molecular characterization of a voltage-gated potassium channel expressed in rat testis. *Mol. Hum. Reprod.*, **6**, 303–313.
9. Arkett, S.A., Dixon, J., Yang, J.N., Sakai, D.D., Minkin, C. and Sims, S.M. (1994) Mammalian osteoclasts express a transient potassium channel with properties of Kv1.3. *Recepts. Channels*, **2**, 281–293.
10. Komarova, S.V., Dixon, S.J. and Sims, S.M. (2001) Osteoclast ion channels: potential targets for antiresorptive drugs. *Curr. Pharm. Des.*, **7**, 637–654.
11. Deutsch, C. and Chen, L.-Q. (1993) Heterologous expression of specific K^+ channels in T lymphocytes: Functional consequences for volume regulation. *Proc. Natl Acad. Sci. USA*, **90**, 10036–10040.
12. Liu, Q.H., Fleischmann, B.K., Hondowicz, B., Maier, C.C., Turka, L.A., Yui, K., Kotlikoff, M.I., Wells, A.D. and Freedman, B.D. (2002) Modulation of Kv channel expression and function by TCR and costimulatory signals during peripheral CD4(+) lymphocyte differentiation. *J. Exp. Med.*, **196**, 897–909.
13. Warntges, S., Friedrich, B., Henke, G., Duranton, C., Lang, A., Waldegger, S., Meyermann, R., Kuhl, D., Speckmann, J., Obermuller, N. *et al.* (2002) Cerebral localization and regulation of the cell volume-sensitive serum- and glucocorticoid-dependent kinase SGK1. *Pflugers Arch.*, **443**, 617–624.
14. Chung, I. and Schlichter, L.C. (1997) Native Kv1.3 channels are upregulated by protein kinase C. *J. Membr. Biol.*, **156**, 73–85.
15. Fadool, D.A., Tucker, K., Phillips, J.J. and Simmen, J.A. (2000) Brain insulin receptor causes activity-dependent current suppression in the olfactory bulb through multiple phosphorylation of Kv1.3. *J. Neurophysiol.*, **83**, 2332–2348.
16. Fadool, D.A. and Levitan, I.B. (1998) Modulation of olfactory bulb neuron potassium current by tyrosine phosphorylation. *J. Neurosci.*, **18**, 6126–6137.
17. Schulingkamp, R.J., Pagano, T.C., Hung, D. and Raffa, R.B. (2000) Insulin receptors and insulin action in the brain: review and clinical implications. *Neurosci. Biobehav. Rev.*, **24**, 855–872.
18. Lowell, B.B. and Spiegelman, B.M. (2000) Towards a molecular understanding of adaptive thermogenesis. *Nature*, **404**, 652–660.
19. Schwartz, M.W., Woods, S.C., Porte, J.D., Seeley, R.J. and Baskin, D.G. (2000) Central nervous system control of food intake. *Nature*, **404**, 661–671.

20. Veh, R.W., Lichtinghagen, R., Sewing, S., Wunder, F., Grumbach, I.M. and Pongs, O. (1995) Immunohistochemical localization of five members of the Kv1 channel subunits: contrasting subcellular locations and neuron-specific co-localizations in rat brain. *Eur. J. Neurosci.*, **7**, 2189–2205.
21. Bruning, J.C., Gautam, D., Burks, D.J., Gillette, J., Schubert, M., Orban, P.C., Klein, R., Krone, W., Muller-Wieland, D. and Kahn, C.R. (2000) Role of brain insulin receptor in control of body weight and reproduction. *Science*, **289**, 2122–2125.
22. Kalra, S.P., Dube, M.G., Pu, S., Xu, B., Horvath, T.L. and Kalra, P.S. (1999) Interacting appetite-regulating pathways in the hypothalamic regulation of body weight. *Endocrine Rev.*, **20**, 68–100.
23. Bolivar, V.J., Cook, M.N. and Flaherty, L. (2001) Mapping of quantitative trait loci with knockout/congenic strains. *Genome Res.*, **11**, 1549–1552.
24. Masuzaki, H., Paterson, J., Shinyama, H., Morton, N.M., Mullins, J.J., Seckl, J.R. and Flier, J.S. (2001) A transgenic model of visceral obesity and the metabolic syndrome. *Science*, **294**, 2166–2170.